The charging stability of different silica glasses studied by measuring the secondary electron emission yield

Zhao Su-Ling(赵谡玲)[a)†] and Bertrand Poumellec[b)‡]

[a)] *Key Laboratory of Luminescence and Optical Information, Beijing Jiaotong University, Ministry of Education, Beijing* 100044, *China*
[b)] *ICMMO/LPCES, UMR CNRS-UPS* 8182, *Université de Paris Sud,* 91405 *Orsay Cedex, France*

(Received 8 December 2009; revised manuscript received 15 October 2010)

This paper reports that the charging properties of lead silica, Suprasil silica and Infrasil silica are investigated by measuring the secondary electron emission (SEE) yield. At a primary electron beam energy of 25 keV, the intrinsic SEE yields measured at very low injection dose are 0.54, 0.29 and 0.35, respectively for lead silica, Suprasil and Infrasil silica glass. During the first e-beam irradiation at a high injection current density, the SEE yields of lead silica and Suprasil increase continuously and slowly from their initial values to a steady state. At the steady state, the SEE yields of lead silica and Suprasil are 0.94 and 0.93, respectively. In Infrasil, several charging and discharging processes are observed during the experiment. This shows that Infrasil does not reach its steady state. Two hours later, all samples are irradiated again in the same place as the first irradiation at a low current density and low dose. The SEE yields of lead silica, Suprasil and Infrasil are 0.69, 0.76 and 0.55, respectively. Twenty hours later, the values are 0.62, 0.64 and 0.33, respectively, for lead silica, Suprasil and Infrasil. These results show that Infrasil has poor charging stability. Comparatively, the charging stability of lead silica is better, and Suprasil has the best characteristics.

Keywords: secondary electron emission yield, charging stability, nonlinear silica glass
PACS: 79.20.Fr, 77.22.Jp, 42.65.Ky **DOI:** 10.1088/1674-1056/20/3/037901

1. Introduction

Electron beam (EB) poling has the advantage that device patterns can be easily fabricated with high spatial resolution, such as the periodically poled structures of a nonlinear optical grating (i.e. $x^{(2)}$ grating) for quasi-phase-matching devices[1] using a computer-aided-design (CAD) system. It has also been shown in several publications that electron irradiation increases the refractive index of various kinds of insulators[2,3] and therefore produces optical waveguides.[4] The e-poling process is considered to produce two electric layers in a sample when it is irradiated. A negative layer is formed beneath the surface when the energy lost by the electron is absorbed. Along the electron path, the particles lose their energy by producing various types of excitation: heat, bond-breaking, densification, microstructure transformations, photoelectrons, Auger electrons i.e. secondary electrons. This last process contributes to charging the atomic layers just beneath the surface of the sample with another charge, which can be positive if the kinetic energy of the electrons is controlled. An internal electric field grows in this way until the breakdown limit is reached. Myers *et al.*[5] published the first report of second-harmonic generation from strongly electrically polarised SiO_2 glasses. Nevertheless, Kazansky *et al.*[6] have shown that electron-beam irradiation does not work on pure silica but erases a second-order nonlinearity in already thermally poled silica. In 1993, Kazansky *et al.*[7]] got a good second order nonlinear coefficient of 0.7 pm/V in lead silica bulk glasses by using the EB poling technique. They observed the absence of a second-harmonic signal in poled lead silica samples with unspecified Pb concentration. This was investigated by Nakanishi *et al.*[7] and Qiu *et al.*[8] who found that the nonlinearity depends not only on the EB current and dose but also on the dopant concentration. However, according to our experience, it is very difficult to get nonlinearity in Infrasil silica glasses poled by EBs. In contrast, it is possible to achieve it in Suprasil silica glasses, but its second order coefficient is very small. Why? Is the trapped charge unstable?

To answer this question, we used secondary electron emission yield (SEEY) measurements to observe the stability of charges after EB irradiation. This method is different to measuring the open-circuit

†E-mail: slzhao@bjtu.edu.cn
‡Corresponding author. E-mail: Bertrand.Poumellec@u-psud.fr
© 2011 Chinese Physical Society and IOP Publishing Ltd

thermally stimulated discharge current–temperature spectrum.[9] The SEEY ($\sigma = I_{\rm sec}/I_0$) parameter is used to determine the sign of the charges in insulating materials submitted to electron irradiation. A study of the charging effect on samples by electron bombardment is not only interesting for stability analysis, but also it reveals information on conduction mechanisms, structure defects, etc.[10] A concern is that, under continued irradiation, the SEEY measurement changes according to electron implantation dose. From low to high doses, we can detect different properties, which reflect the internal built-in electric field. When the EB is stopped, the charge is unstable if the SEEY changes during this period of time. In our work, we measured the charging stability of different silica glasses analysed by SEEY.

2. Experiments

The samples consist of Suprasil silica, Infrasil silica and lead silica glasses. In order to clean their surface from water, the samples were annealed in an argon atmosphere at 400 °C for 1 hour before mounting on the sample holder inside a Secondary Electron Microscope (SEM).

The experiments were performed with an SEM Predictscan LEO 440 equipped with the optibeam optical system which allows the beam to be focused at a fixed position (point A' in Fig. 1) after the second magnetic condenser lens for any energy and current intensity required as shown in Ref. [11]. The EB blanking unit (EBBU) is composed of two plates centred at point A, in order to avoid the lateral displacement of the beam during the blanking operation. The EBBU is activated by a function generator, which allows the delivering of pulses varying from 10^{-3} s to 40 s with a dose adjustable from a few 10^{-2} pC/pulse to calibrated 10^8 pC/pulse.

A Faraday cup is used to calibrate the injected current I_0 that relates with the injected dose Q_0 before irradiating the sample. A collector called SB allows measuring the dose $Q_{\rm SB}$ corresponding to secondary and backscattered electrons. Backscattered electrons are due to elastic scattering of primary electrons in the sample whereas secondary electrons arise from inelastic collisions between primary electrons and the material atoms. What we call the total secondary electron emission intensity, usually is the sum of both contribution, it is detected by the SB collector, and denoted as $I_{\rm SB}$. The induced current $I_{\rm IC}$, measured during a given period of time, corresponds to the number of electrons ($Q_{\rm IC}$ is the induced dose) accumulated in the sample. The detailed experimental set-up is shown in Ref. [11]. According to the Kirchoff current law, the primary EB current I_0 must equal the sum $I_{\rm IC}+I_{\rm SB}$ if no electrons are lost on the way to the sample. However, when charges are trapped locally, the surface potential increases and deviates the beam producing a mirror effect.[12] In that case, $I_{\rm IC}+I_{\rm SB} < I_0$. The SEEY σ is given by $\sigma = I_{\rm SB}/(I_{\rm SB}+I_{\rm IC})$.

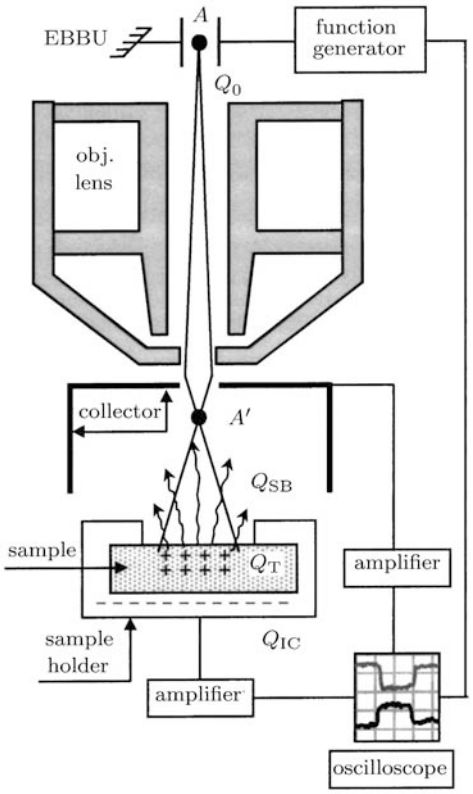


Fig. 1. Scheme of the bottom part of the microscope and principle of the induced current and secondary electron emission measurements. The $Q_{\rm IC}$ is the induced charge, $Q_{\rm T}$ the trapped charge, and $Q_{\rm SB}$ the secondary and backscattered electron charge.[11] The induced charge is produced in the surrounding shield by influence. After calibration, $Q_{\rm T} = Q_{\rm IC}$.

The experiments were carried out in the spot mode by defocusing the electron beam of SEM and by irradiating the sample surface with a sequence of short electron pulses. The 3 samples were fixed together on the SEM sample holder in order to conserve the same experimental conditions for allowing comparisons. Then the sample cavity was kept under vacuum for all set of experiments. The thickness of all samples was more than 1 mm. The EB diameter on the sample surface is fixed at 455.5 μm and the charge injection pulse duration was controlled from 0.01 to 10 s.

The primary electron energy was 25 keV. This energy is higher than the energy $E_{c2} \cong 3000$ eV (for silica glass) of the second cross-over for which σ (E_{c2})=1. So σ(25 keV)< 1 and all the samples were charged negatively.[13]

Two sets of experimental conditions specified in Table 1 were used: a large incident beam current and injected dose in order to charge the sample, and a low current and dose for σ measurements.

3. Experimental Results

3.1. Intrinsic SEEY σ_0 at 25 keV

The intrinsic yield σ_0 is obtained at a low current, with a large beam size and short beam pulse as shown in Table 1. Under these conditions, the two signals sent by the electrons to the material and the sum of the implanted and emitted electrons are complementary as shown in Fig. 2 for the lead silica sample.

Table 1. Experimental parameters.

operation	primary energy	beam current	diameter of electron beam	current density	irradiation time	injected dose
σ measurement	25 keV	40.0 pA	455.5 μm	2.5×10^4 pA/cm^2	1 s	2.5×10^4 pC/cm^2
charging stability measurement	25 keV	4.00 nA	455.5 μm	2.5×10^6 pA/cm^2	10 s	2.5×10^7 pC/cm^2

Before the experiment, the beam current was calibrated with a precision of 0.5 %, that is $I_0 = 40.0 \pm 0.2$ pA. During the experiment, the total current $I_{IC}+I_{SB}$ remained equal to the calibrated current within this precision.

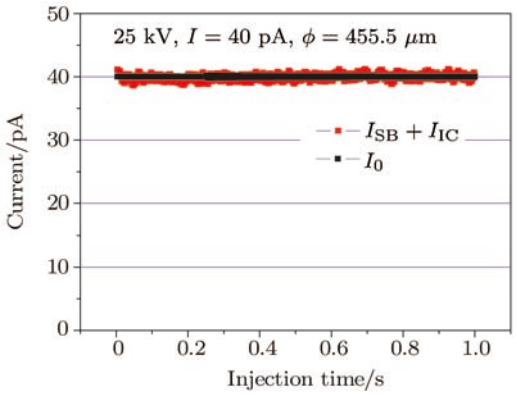


Fig. 2. (Colour online) Variation of the injected current with time, during the intrinsic SEEY measurement at 25 kV in lead silica.

Figure 3 shows the kinetics for σ_0. The injection dose of 2.5×10^4 pC/cm^2 for every sample is low enough such that the obtained yield corresponds to the intrinsic yield of the uncharged sample. After averaging the value at the beginning of the irradiation, we got the intrinsic values of σ_0 recorded in Table 2.

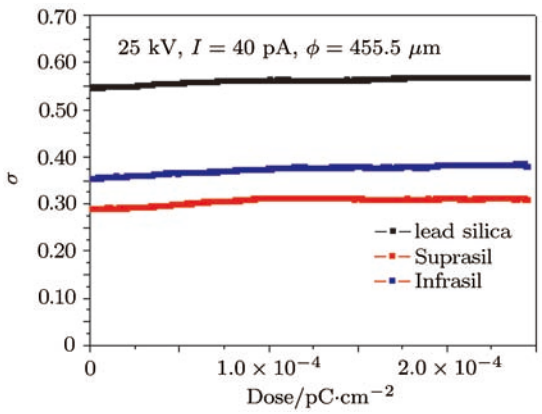


Fig. 3. (Colour online) Intrinsic SEEYs of lead silica, Suprasil and Infrasil silica at 25 kV with very low dose.

Table 2. Produced $\chi^{(2)}$ by e-poling in different samples and different σ at 25 keV.

sample	$\chi^{(2)}$/(pm/V)	σ_0	$\sigma_{\text{steady state}}$/4nA	$\sigma_{\text{2h later}}$/40pA	$\sigma_{\text{20h later}}$/40pA
Suprasil	small by e-poling	0.29	0.93	0.76	0.64
Infrasil	No by e-poling	0.35	Unstable	0.55	0.33
lead silica	0.7 by e-poling[7]	0.54	0.94	0.69	0.62

Note: The $\chi^{(2)}$ of Suprasil and Infrasil were detected by additional experiments under the same e-poling conditions, and that of Lead silica refered from Ref. [7].

3.2. Charge stability measurements

3.2.1. Lead silica and Suprasil silica

The variation of σ with injection dose was measured by using the charging conditions specified in Table 1. After the charging operation, all the samples were kept in the SEM chamber under a high vacuum. Two hours and 20 hours later, σ was measured again with a lower current density and dose (σ measurements in table 1) at the same place after being charged by the first irradiation. In this experiment, the injection charge is sufficiently low that the obtained yield σ during this shot corresponds to the unperturbed yield of the charged sample.

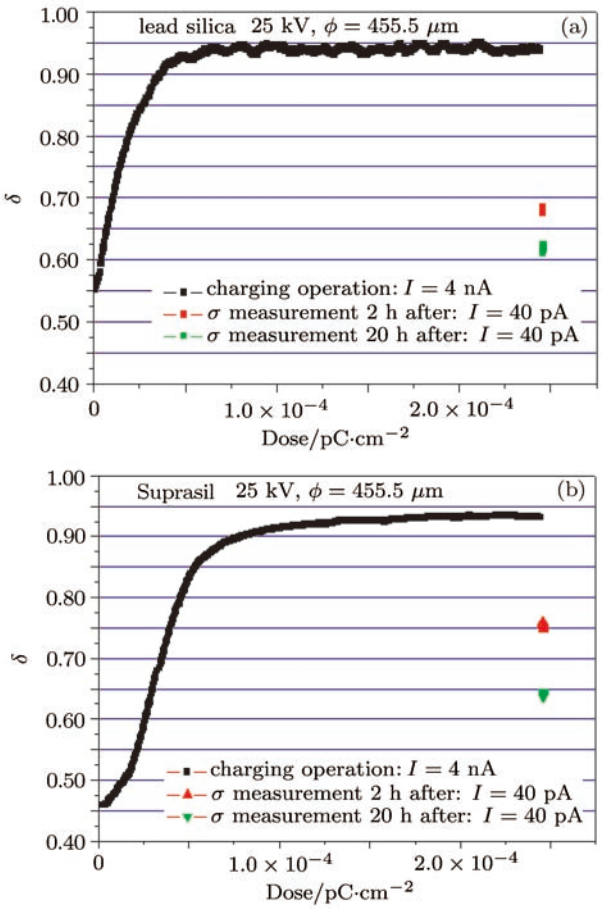


Fig. 4. (Colour online) The variation of yield σ at 25 kV according with injected dose (black); σ measured 2 hours later at low current density and low injected dose (red); σ measured again, 20 hours later (green). (a) lead silica; (b) suprasil silica glass.

The results for the lead silica and Suprasil silica are shown in Figs. 4(a) and 4(b), respectively. During charging, the SEEY increases continuously and rapidly from its initial value to steady values of $\sigma = 0.94$ and 0.93, respectively. It is necessary to inject a very high dose in order to reach the steady state as seen in Fig. 4: about 6.5×10^6 pC/cm^2 for lead silica and 1.7×10^7 pC/cm^2 for Suprasil. Two hours later, the yield does not stay at the steady value close to unity, obtained at the end of the charging process (Table 2): it reduces to 0.69 in lead silica and to 0.76 in Suprasil. Twenty hours later, they have decreased much further to 0.61 in lead silica and to 0.64 in Suprasil.

Figure 5 shows the current changes in lead silica during the σ measurements, 2 hours and 20 hours after charging. The total current ($I_{IC} + I_{SB}$) is not strictly equal to I_0 as was the case in Fig. 2. The differences between the total sum and I_0 are 4 pA and 2 pA, respectively. These results clearly show that the sample has been strongly charged first, producing a mirror effect that impedes the collection of secondary electrons.

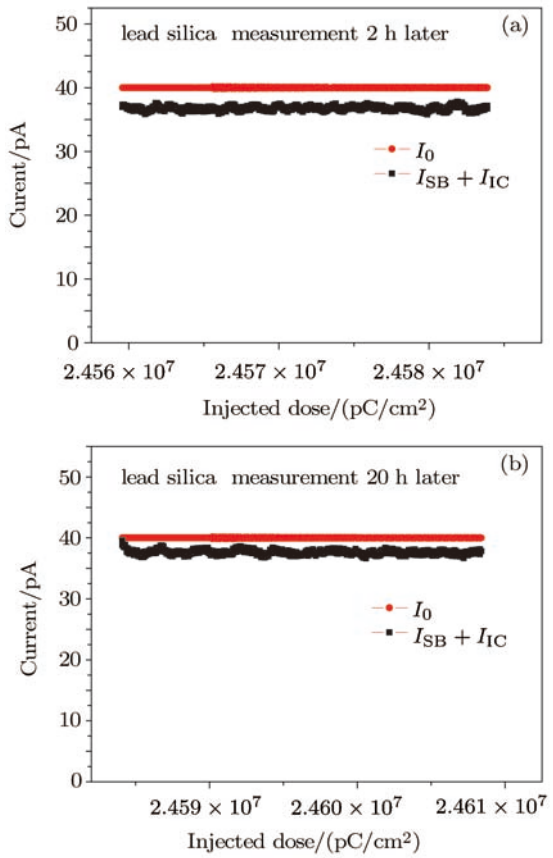


Fig. 5. (Colour online) Correspondence between the real current $I_{IC} + I_{SB}$ and calibrated current I_0 during the σ measurements at 25kV in lead silica: (a) 2 hours after charging; (b) 20 hours after charging.

3.2.2. Infrasil silica glass

Figure 6 shows the evolution of the yield σ of Infrasil silica with injection dose. All the experimental parameters are the same as those used on the

other two samples. After a regular increase at the beginning of injection, σ exhibits a short plateau before rising rapidly to unity and dropping down to a low value (0.47) only slightly higher than the intrinsic value (0.35). As injection progresses, the evolution of σ exhibits three other large peaks with a maximum close to unity and a minimum closer to the intrinsic value, and a fourth smaller peak before stabilizing to a value of 0.4. After 2 hours, $\sigma = 0.55$ and finally after 20 hours $\sigma = 0.33$, which is almost equal to the intrinsic value. It seems that the steady state cannot be achieved in this sample, it behaves like an uncharged material.

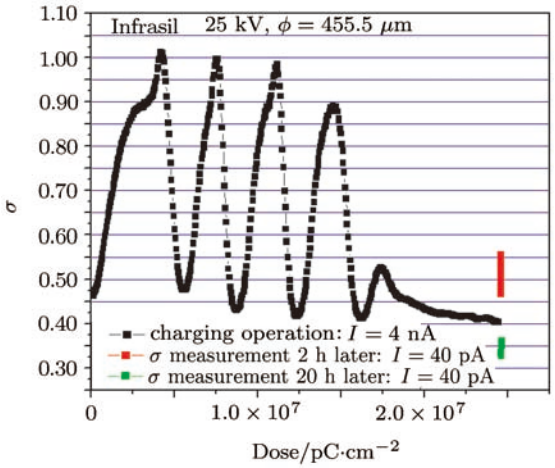


Fig. 6. (Colour online) The variation of σ in infrasil silica with the injected dose (black). The σ values measured at low current density and low injected dose 2 hours later (red) and 20 hours later (green).

The integrated dose $Q_s = \Sigma\ (I_{IC} + I_{SB})\ \Delta t$ as a function of the injected dose $Q_i = \sum I_0\ \Delta t$ shows a straight line with a one-to-one correlation. Good agreement is achieved from the beginning to the end of the charging operation (Fig. 7). In the middle, the total current departs only slightly from I_0 during the charging and discharging parts of the cycle.

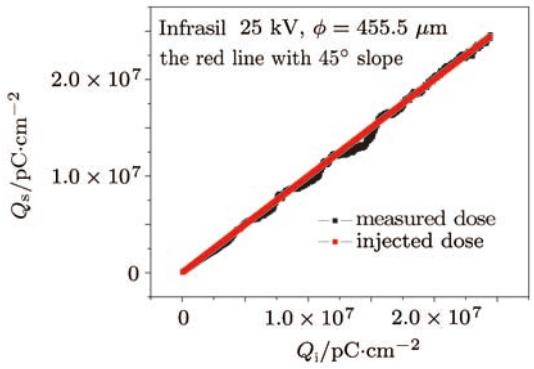


Fig. 7. (Colour online) Measured dose $Q_s = \Sigma\ (I_{IC}+I_{SB})$ Δt as a function of the injected dose $Q_i = \Sigma I_0 \Delta t$ in Infrasil silica during the charging operation.

4. Discussion

The intrinsic yield σ_0 is obtained at 25 kV with low current density. The value obtained for σ_0 is different between samples. This is because the intrinsic yield σ_0 is related to material composition. The difference between Suprasil and Infrasil is likely due to the different water content between these two grades of silica. For lead silica glass, its intrinsic yield σ_0 is mainly determined by lead content, a heavy element.

The variation of the total electron emission yield σ with injection at 25kV is similar for lead silica and Suprasil silica during the first irradiation stage. It is noticeable that both samples were charged negatively with a high primary beam energy ($E = 25$ keV). The coefficient σ starts from its initial value and reaches a plateau before the end of the first irradiation. The initial coefficient σ of both samples is different from their individual intrinsic values σ_0 at the same primary beam energy. This phenomenon has been reported and is due to the different injection current density.[14] When σ reaches the plateau value, we say that charging of the sample has reached a steady state. The process before reaching the steady state reveals the charging properties of the metal. In Figs. 4(a) and 4(b), it can be seen that Suprasil silica needs a higher dose than lead silica to reach its steady state. The slow change of σ before reaching saturation in Fig. 4(b) reveals that traps have been created by electron beam irradiation. The dose at which a steady state is reached depends on the trapping ability of the material. When the dose is small, this means that there are sufficient traps to trap incoming electrons, and conversely, when the dose is large this means that traps are created at the same time as incoming electrons are trapped.[15] The first case seems better for electron poling. After 6.5×10^6 pC/cm^2 has been injected, lead silica reaches its steady state. And after 2×10^7 pC/cm^2 has been injected, Suprasil has only just reached its steady state. By comparing the charging properties, it is concluded that lead silica is better than Suprasil silica for EB poling. Moreover, our experiments which will be published in another paper have demonstrated that the $\chi^{(2)}$ of Suprasil poled by the EB is smaller than that of EB poled lead silica.

After samples reach their individual steady states, they are characterized by a static space charge that is independent of injected charge. It is composed by a positive layer at the surface (100 nm beneath it, in fact) and a negative one below, deep in the material.

The positive layer is a hole layer induced by releasing secondary electrons to the vacuum. The negative layer is made up by trapping primary electrons. This space charge is stable if the conductivity after irradiation of the sample are not sufficient to neutralize them. At an acceleration energy of 25 kV, primary electrons losing their energy on the way stopped around 5 microns below the sample surface according to the following formula:[16]

$$R(\mu\text{m}) = \frac{0.0276 \cdot A \cdot E_0^{5/3}}{\rho \cdot Z^{8/9}} \beta(E_0),$$

where

$$\beta(E_0) = \frac{(1 + 0.978 \cdot 10^{-6} \cdot E_0)^{5/3}}{(1 + 0.957 \cdot 10^{-6} \cdot E_0)^{4/3}},$$

A is the atomic weight, ρ is the density of the sample, Z is the atomic number, and E_0 is the primary electron energy. For a compound, we should use the effective atomic number Z_{eff} calculated from the formula:[17]

$$Z_{\text{eff}} = \sqrt[2.94]{f_1 \times (Z_1)^{2.94} + f_2 \times (Z_2)^{2.94} + f_3 \times (Z_3)^{2.94} + \ldots},$$

where f_n is the fraction of the total number of electrons associated with each element, and Z_n is the atomic number of each element. For silica glass (SiO_2), Z_{eff} is about 10.8. A, that is the molecular weight of SiO_2 is 60, ρ is 2.65 g/cm^3 for silica glass. If $E_0 = 25$ keV, the penetration depth in silica glass is about 5 microns.

The positive and negative charges do not balance as globally the sample is charged negatively. This negative charge corresponds to an electric field which acts to block the primary electron injection, leading to an increase of σ that reaches unity. At this stage, one secondary electron is emitted for each injected primary electron. If the charge trapped in the sample is stable, that is the internal electric field is stable, the yield coefficient σ should not change with time afterwards even if we stop the irradiation. In the reversed case, SEEY decreases towards the intrinsic value.

For performing the test, we measured the yield coefficient σ after charging operation at the same place after 2 hours and 20 hours of blanking, but with an injected current density and injected dose as low as possible. The σ of the charged samples appears to have decreased in comparison to the value of σ at the end of the first irradiation. The difference in the yield coefficient σ results in a difference in conductivity corresponding to de-trapping of charges. After 2 hours, the yield of lead silica is 0.69 and that of Suprasil is 0.76. This corresponds to a migration of charge of 5.47×10^6 pC/cm^2 and 1.6×10^7 pC/cm^2, respectively, for lead silica and Suprasil. After a wait of 20 hours values are 0.61 and 0.64 for lead silica and Suprasil, respectively. The corresponding migration of charge are 6.0×10^6 pC/cm^2 and 1.7×10^7 pC/cm^2 respectively. The remaining dose densities in lead silica and Suprasil are 5×10^5 pC/cm^2 and 3×10^6 pC/cm^2, respectively, which means that about 8% and 15% of the charges remain. We conclude that the charging stability of Suprasil and of lead silica is poor.

The surface field produced by the remaining trapped charge and responsible for χ^2 can be estimated from a classical electrostatic formulation. After 20 hours, the remaining charge density in lead silica is 5×10^5 pC/cm^2. Therefore, the internal electric field E in lead silica is E=dose density/ε=5.65×10^8 V/m. For Suprasil, the internal electric field is about 3.32×10^9 V/m. The nonlinear coefficient d_{33} depends on the internal electric field E as $d_{33} = 3/2\chi^3 E$, and $\chi^3 = 1.6 \times 10^{-21}$ (m/V)^2 for silica glass. For lead silica, when the internal electric field E is equal to 5.65×10^8 V/m, then $\chi^2 = 2d_{33} = 1.8$ pm/V and, for Suprasil, $E = 3.32 \times 10^9$ V/m, $\chi^2 = 2d_{33} = 5.3$ pm/V. This quantity is about one order of magnitude overestimated.

In the virgin sample during electron irradiation, the measured current $I_{\text{SB}} + I_{\text{IC}}$ is equal to I_0 as shown in Fig. 2. This is because the injected dose is very low and the negative surface potential is small. After charging, the current sum, $I_{\text{BC}} + I_{\text{IC}}$, is not equal to the injection current I_0 as shown in Figs. 4(a) and 4(b). So where are the other electrons? The difference between the summed current and I_0 must be due to a partial mirror effect. Electrons trapped by the sample during the charging period produce a mirror effect and a repulsive force which acts against the injected electrons. The surface potential is very high in Suprasil and lead silica after this operation and some electrons escape the collector SB. The consequence is an error of a few percent on the yield (see Fig. 5). After 20 hours, the current dispersed by the mirror effect

becomes smaller. This is because of the reduction of the mirror effect thanks to the migration of trapped charges in the sample.

The charging kinetics of lead silica and Suprasil are typical of insulators in which charges are stabilized for a much longer time than the injection time which is some tens of minutes in the present case. In contrast, the behaviour of Infrasil is characteristic of charge instability. When the internal field reaches a critical value, a large explosion occurs, carrying away a large fraction of the trapped charges. During the first irradiation, several charging and discharging processes were observed, as shown in Fig. 6. The process is reproduced quasi regularly with a certain amount of damping due to the filling up of material with charges. It seems that Infrasil cannot carry so much injected charge. The charging and discharging processes indicate unstable charging. Finally, at the end of the first irradiation, the yield we obtained is close to the intrinsic value and does not change anymore with injected dose. It seems that some conduction can take place in Infrasil, probably due to the internal field. Usually, during the phase expansion of the charge distribution, an exo-emission is observed which produces intense and narrow pulses of electrons. This is not the case here because charges are concentrated deeply and the relaxation is too slow to produce intense peaks (Fig. 6).

It is known that the SEEY of a metal does not change when the injected dose is increased due to its high conductivity. After being irradiated in the first experiment, Infrasil behaves more like a metal with high conductivity. There is no trapped charge remaining in the sample. The result is that there is no mirror effect. Therefore, the total sum at the end of this irradiation is much like the current at the beginning and is equal to I_0. This is illustrated in Fig. 7. After 2 hours or 20 hours, although the yield is different to that at the end of the first irradiation, the sum of $I_{\rm SB}$ and $I_{\rm IC}$ is still equal to the injected current. This means that there is no mirror effect during these two experiments, that is, there are no trapped charges in Infrasil after the first irradiation. So, it is impossible to get second harmonic generation (SHG) signal by EB poling in this sample.

5. Conclusion

The charging stability of lead silica, Suprasil and Infrasil was studied by SEEY measurement. At 25 kV, the intrinsic SEEY values of lead silica, Suprasil and Infrasil are 0.54, 0.29 and 0.35, respectively.

The variation of the yield σ along with the injected dose was measured in three samples with the same experimental parameters. Infrasil experienced several charging and discharging processes during the SEEY measurements. The charging stability of this material is very poor. At the end of the first irradiation, Infrasil behaves like a conducting material with quite a high conductivity. It is thus impossible to obtain SHG in Infrasil silica by EB poling.

In the steady state, the SEEY values of lead silica and Suprasil are 0.94 and 0.93, respectively. Two hours and 20 hours after the first irradiation, the SEEY values are 0.69 and 0.62 for lead silica, and 0.76 and 0.64 for Suprasil. The decay of the SEEY value indicates unstable charging. The current deflected by the mirror effect helps explain this result.

In summary, the sample with most stable charging characteristics is Suprasil, while the next best is lead silica. The worst is Infrasil. It is possible to obtain SHG in Suprasil and lead silica by an EB. There are a sufficient number of traps to capture incoming electrons during EB irradiation in lead silica. However, in Suprasil, the traps have to be created by the irradiation itself. From the earlier discussion, it is concluded that lead silica is better than Suprasil silica for obtaining SHG by electron beam poling.

This set of experiments allows to differentiate insulating samples chosen *a priori* for EB poling. The electric fields created are high and thus it is a suitable method for investigating the insulating properties under high electric fields. This method can also be applied to investigations of poling stability achieved by e displacement by means of ultraviolet or x-ray irradiation.

Acknowledgement

A special acknowledgement should be shown to Professor Guy Blaise, from whose experimental support and discussion we benefited greatly. This work was supported by the European Commission in the framework of the GLAMOROUS contract (ref. IST 2000-28366).

References

[1] Hsu W Y and Gupta M C 1992 *Appl. Phys. Lett.* **60** 1

[2] Barbier D, Green M and Madden S J 1991 *J. Lightwave Technol.* **9** 715

[3] Garcia Blanco S, Glidle A, Davies J H, Aitchison J S and Cooper J M 2001 *Appl. Phys. Lett.* **79** 2889

[4] Syms R R A, Tate T J and Lewandowski J J 1994 *J. Lightwave Technol.* **12** 2085

[5] Myers R A, Mukherjee N and Brueck S R J 1991 *Opt. Lett.* **16** 1732

[6] Kazansky P G, Kamal A and Russell P St J 1993 *Opt. Lett.* **18** 1141

[7] Kazansky P G, Kamal A and Russell P St J 1993 *Opt. Lett.* **18** 693

[8] Qiu M, Pi F and Orriols G 1998 *Appl. Phys. Lett.* **73** 3040

[9] Cheng G J, Xia Z F, Zhang Y W and Zhang H Y 1999 *Acta Phys. Sin.* **48** 1676 (in Chinese)

[10] Cazaux J, Kim K H, Jbara O and Salace G 1991 *J. Appl. Phys.* **70** 960

[11] Braga D, Poumellec B, Cannas V, Blaise G, Ren Y and Kristensen M 2004 *J. Appl. Phys.* **96** 885

[12] Vallayer B, Blaise G and Treheux D 1999 *Rev. Scientific Instrum.* **70** 3102

[13] Liebault J, Zarbout K, Moya G and Kallel A 2003 *Journal of Non-Crystalline Solids* **322** 213

[14] Thome T, Braga D and Blaise G 2004 *J. Appl. Phys.* **95** 2619

[15] Cazaux J 2004 *J. Appl. Phys.* **95** 731

[16] Feldman C 1960 *Phys. Rev.* **117** 455

[17] Murty R C 1965 *Nature* **207** 398